A lifting scheme of biorthogonal wavelet transform based on discrete interpolatory splines

Amir Z. Averbuch[a] Alexander B. Pevnyi[b] and Valery A. Zheludev [a]

[a]Department of Computer Science, Tel Aviv University
Tel Aviv 69978, Israel
[b]Department of Mathematics, Syktyvkar University, Syktyvkar, Russia

ABSTRACT

In the paper we present a new family of biorthogonal wavelet transforms and a related library of biorthogonal periodic symmetric waveforms. For the construction we used the interpolatory discrete splines which enabled us to design a library of perfect reconstruction filter banks. These filter banks are related to Butterworth filters. The construction is performed in a "lifting" manner. The difference from the conventional lifting scheme is that all the transforms are implemented in the frequency domain with the use of the fast Fourier transform (FFT). Two ways to choose the control filters are suggested. The proposed scheme is based on interpolation and, as such, it involves only samples of signals and it does not require any use of quadrature formulas. These filters have linear phase property and the basic waveforms are symmetric. In addition, these filters yield perfect frequency resolution.

Keywords: Discrete splines, biorthogonal wavelets, lifting scheme, Butterworth filters

1. INTRODUCTION

The continuous polynomial splines has a rich history as a source for wavelet constructions: Refs 2, 7, 3, 14, 4, 15. But only a few authors use the discrete splines for this purpose (Refs. 8, 11). However, discrete splines is a natural tool for processing of discrete time signals. An intermediate approach can be found in Ref. 1 where the authors used the filters that originated from the discretized B-splines for the construction of the multiresolution analysis in the space l_2.

In this work we employed the interpolatory periodic discrete splines (Ref. 9) as a tool for devising a fully discrete biorthogonal wavelet scheme. The proposed construction is somewhat related to Donoho's interpolating wavelet construction Ref. 5 as it was modified later by Sweldens Ref. 13 into what is called the "lifting scheme". The lifting scheme allows custom design and fast implementation of the transforms. Briefly, the idea of the computation is that values of the signal located at odd positions are predicted by values in the midpoints of the spline that interpolates the even values of the signal. Then, the odd subarray is replaced by the difference between the current and the predicted subarrays. On smooth well-correlated fragments of the signal, these differences will be near zero whereas irregular fragments will produce significant differences. This result resembles the operation of the wavelet transform. To further extend this resemblance we should employ the new odd subarray for updating the existing even subarray. The goal of this update is to smooth the even subarray and thus reduce the aliasing which is a consequence of decimation. Based upon the above strategy, we constructed a new family of biorthogonal wavelet and wavelet packet transforms and a related library of biorthogonal symmetric waveforms. In Ref. 15 a similar approach was conducted through the use of polynomial interpolatory splines as the predicting aggregate. In that paper as well as in the present one all the computations are conducted in the frequency domain using FFT.

Our construction resulted in a perfect reconstruction filter bank with linear phase filters. The corresponding wavelets are symmetric. The constructed filter banks comprise filters which act as a two-passes (forward and backward) half-band Butterworth filters (Ref. 10) and the filters dual to them. The frequency response of Butterworth filters are maximally flat and we succeeded in construction of dual filters with similar property.

Further author information: (Send correspondence to Valery A. Zheludev)
Valery A. Zheludev : E-mail: zhel@math.tau.ac.il
Amir Z. Averbuch: E-mail: amir@math.tau.ac.il
Alexander B. Pevnyi: E-mail: pevnyi@ssu.edu.komi.com

The one-pass Butterworth filters were used already for devising an orthogonal non-symmetric wavelets Ref. 6. The computations there were conducted in the time domain using recursive filtering. Note, that the same can be done in our scheme.

The paper is organized as follows: In section 2 we outline some facts about the discrete splines. In section 3 we devise a family of biorthogonal wavelet-type transforms of signals using lifting steps. The lifting scheme that we propose operates in the frequency domain contrary to the conventional lifting scheme. Both the primal and dual schemes for construction are considered. We emphasize the fact that the lifting scheme together with the proposed construction yields an efficient computational algorithm. Section 4 is devoted to the description of the properties of the constructed filter banks and basic elements of the transforms. The filter banks contain some control tools which supply the scheme with means for flexible adaptation. In the end of the section we show how to use these control tools.

The transforms that were presented in section 3 are one-level (scale) wavelet-type transforms. They can be decomposed into more scales in two ways. One is the multiscale wavelet transform when the frequency domain is splitted in line with the logarithmic scale. Another way is the wavelet packet transform when the partition of the frequency domain is near uniform and it is being refined in each subsequent scale of the transform. We describe in Section 5 the wavelet type transform. Throughout the paper we present a wide collection of filter banks, wavelets and their spectra.

2. PRELIMINARIES

In this section we outline briefly the properties of discrete periodic splines which are needed for further constructions. For detailed description of the subject see Ref. 9.

Throughout the paper we assume that m, n and t are natural numbers and $mn = N = 2^t$. Denote $\omega_N = e^{2\pi i/N}$. The discrete Fourier transform (DFT) of an array $\{a(k)\}_{k=0}^{N-1}$ and its inverse (IDFT) $\{\widehat{a}(j)\}_{j=0}^{N-1}$ are

$$\widehat{a}(j) = \sum_{k=0}^{N-1} \omega_N^{-jk}\, a(k), \qquad a(k) = \frac{1}{N} \sum_{j=0}^{N-1} \omega_N^{jk}\, \widehat{a}(j), \quad j,k = 0,\dots,N-1.$$

Definition 2.1. *The IDFT of the sequence*

$$q_{r,m,n}(j) = \begin{cases} n^{2r} & \text{if } j = 0 \\ \left(\frac{\sin \pi j/m}{\sin \pi j/N}\right)^{2r} & \text{if } j = 1,\dots N-1 \end{cases} \quad : \quad Q_{r,m,n}(k) = \frac{1}{N} \sum_{j=0}^{N-1} \omega_N^{jk} q_{r,m,n}(j). \tag{2.1}$$

is called the (m,n) discrete periodic B-spline of order $2r$. The (m,n) discrete periodic spline of order $2r$ is defined as a linear combination, with real-valued coefficients, of shifts of the (m,n) B-spline of order $2r$:

$$S_{r,m,n}(k) = \sum_{l=0}^{m-1} c(l) Q_{r,m,n}(k - nl). \tag{2.2}$$

In the paper we are interested only in the case when $m = N/2$ and $n = 2$. The corresponding splines are denoted as $Q_r = Q_{r,N/2,\,2}$ and $S_r = S_{r,N/2,\,2}$. In this case we have

$$Q_r(k) = \frac{1}{N} \sum_{j=0}^{N-1} \omega_N^{jk} \left(2\cos\frac{j\pi}{N}\right)^{2r}, \quad S_r(k) = \sum_{l=0}^{m-1} c(l) Q_r(k-2l). \tag{2.3}$$

Definition 2.2. *The discrete spline is called the interpolatory spline if the following relations hold:*

$$S_r(2k) = e(k),\ k \in 0,\dots,m-1. \tag{2.4}$$

The $\{2k\}$ points are called the nodes of the spline.

Any interpolatory splines of any order can be explicitly constructed, but for further development we need to know the values of the splines in the midpoints between the nodes, which we denote as $\sigma(k) = S_r(2k+1),\ k \in 0, \ldots, m-1$.

PROPOSITION 2.3. *The values of the interpolatory spline in the midpoints are*

$$\sigma(k) = \frac{1}{m} \sum_{j=0}^{m-1} \omega_m^{jk} \widehat{\sigma}(j), \quad \widehat{\sigma}(j) = \widehat{e}(j)\omega_N^j U_1(j), \quad U_1(j) = \frac{\left(\cos\frac{j\pi}{N}\right)^{2r} - \left(\sin\frac{j\pi}{N}\right)^{2r}}{\left(\cos\frac{j\pi}{N}\right)^{2r} + \left(\sin\frac{j\pi}{N}\right)^{2r}}, \quad j,\, k = 0, \ldots, m-1. \tag{2.5}$$

The function U_1 is N-periodic and $U_1(j+m) = -U_1(j)$.

3. BIORTHOGONAL TRANSFORMS

We introduce a family of biorthogonal wavelet-type transforms for the signal $\mathbf{z} = \{z(k)\},\ k = 0, \ldots N-1$, which we construct through the lifting steps. The significant difference with the conventional lifting scheme Ref. 13 lies in the fact that here we operate in the frequency domain.

The lifting scheme can be implemented in a primal or dual modes. We consider both.

3.1. Primal scheme

3.1.1. Decomposition

Generally, the lifting scheme for decomposition of signals consists of three steps: 1. Split. 2. Predict. 3. Update or lifting. Let us construct and implement our proposed schemes in terms of these steps.

Split - This is the easiest operation. We simply split the array $\mathbf{z}$ into an even and odd sub-arrays:

$$\mathbf{e_1} = \{e_1(k) = z(2k)\}, \quad \mathbf{d_1} = \{d_1(k) = z(2k+1)\},\ k \in 0, \ldots, m-1;\ m = N/2.$$

Predict - We use the even array $\mathbf{e_1}$ to predict the odd array $\mathbf{d_1}$ and redefine the array $\mathbf{d_1}$ as the difference between the existing array and the predicted one.

To be specific, we use the spline S_r which interpolates the sequence $\mathbf{e_1}$ and predict the array $\widehat{\mathbf{d}}_1$. The array $\widehat{\mathbf{d}}_1$, which is the DFT of $\mathbf{d_1}$, is predicted by the array $\widehat{\sigma}$ defined in (2.5). The DFT of the new $d-$array is defined as follows:

$$\widehat{d}_1^u(j) = \widehat{d}_1(j) - \widehat{e}_1(j)\omega_N^j U_1(j),\ j \in 0, \ldots, m-1. \tag{3.1}$$

From now on the superscript u means *update* of the array.

Lifting - We update the even array using the new odd array:

$$\widehat{e}_1^u(j) = \widehat{e}_1(j) + \beta_1(j)\omega_N^{-j}\, \widehat{d}_1^u(j), \tag{3.2}$$

where $\beta_1(j)$ is a real-valued $N-$periodic sequence obeys the condition $\beta_1(j+m) = -\beta_1(j)$.

3.1.2. Reconstruction

The reconstruction of the signal $\mathbf{z}$ from the arrays $\mathbf{e_1^u}$ and $\mathbf{d_1^u}$ is implemented in reverse order: 1. Undo Lifting. 2. Undo Predict. 3. Unsplit.

Undo Lifting - We restore immediately the even array:

$$\widehat{e}_1(j) = \widehat{e}_1^u(j) - \beta_1(j)\omega_N^{-j}\, \widehat{d}_1^u(j), \tag{3.3}$$

Undo Predict - We restore the odd array:

$$\widehat{d}_1(j) = \widehat{d}_1^u(j) + \widehat{e}_1(j)\omega_N^j U_1(j),\ j \in 0, \ldots, m-1. \tag{3.4}$$

Let us rewrite Eq. (3.4) using Eq. (3.3).

$$\begin{aligned} \widehat{d}_1(j) &= \widehat{d}_1^u(j) + \omega_N^j U_1(j) \left(\widehat{e}_1^u(j) - \beta_1(j)\omega_N^{-j}\, \widehat{d}_1^u(j)\right) \\ &= \widehat{d}_1^u(j) \left(1 - \beta_1(j)\omega_N^{-j} U_1(j)\right) + \omega_N^j U_1(j)\, \widehat{e}_1^u(j). \end{aligned} \tag{3.5}$$

Unsplit - The last step represents the standard restoration of the signal from its even and odd components. In the frequency domain it looks as:

$$\widehat{z}(j) = \widehat{e_1}(j) + \omega_N^{-j}\widehat{d}_1(j), \quad j = 0, \ldots, N-1. \tag{3.6}$$

3.2. Dual scheme

In the primal construction, that was described above, the update step is controlled by the function $\beta_1(j)$. Now we explain the dual scheme where the prediction step is under control.

3.2.1. Decomposition

1. We start by averaging the even array with its prediction that was derived from the odd array:

$$\widehat{e}_1^u(j) = \frac{1}{2}\left(\widehat{e}_1(j) + \omega_N^{-j}\, U_1(j)\widehat{d}_1(j)\right). \tag{3.7}$$

   Such an update results in a smoother even array.

2. We form the details array by extracting from the odd array the new even array supplied with the control function $\beta_1(j)$:

$$\widehat{d}_1^u(j) = \widehat{d}_1(j) - 2\beta_1(j)\omega_N^j\, \widehat{e}_1^u(j). \tag{3.8}$$

3.2.2. Reconstruction

1. We restore the odd array

$$\widehat{d}_1(j) = \widehat{d}_1^u(j) + 2\beta_1(j)\omega_N^j\, \widehat{e}_1^u(j).$$

2. To reconstruct the even array we use $\widehat{d}_1(j)$:

$$\hat{e}_1(j) = 2\widehat{e}_1^u(j) - \omega_N^{-j}U_1(j)\widehat{d}_1(j).$$

3. Finally,

$$\widehat{z}(j) = \widehat{e_1}(j) + \omega_N^{-j}\widehat{d}_1(j), \quad j = 0, \ldots, N-1.$$

4. FILTER BANKS AND RELATED BASES

4.1. Filter banks

Lifting schemes, that were presented above, yield efficient algorithms for the implementation of the forward and backward transform of $\mathbf{z} \longleftrightarrow \mathbf{e_1^u} \cup \mathbf{d_1^u}$. But these operations can be interpreted as transformations of the signals by a filter bank that possesses the perfect reconstruction properties.

THEOREM 4.1. *Define the $N-$periodic functions*

$$\tilde{g}^1(j) = \omega_N^{-j}\Big(1 - U_1(j)\Big) = \omega_N^{-j}\frac{2\left(\sin\frac{j\pi}{N}\right)^{2r}}{\left(\cos\frac{j\pi}{N}\right)^{2r} + \left(\sin\frac{j\pi}{N}\right)^{2r}},\ j \in 0, \ldots, N, \tag{4.1}$$

$$\tilde{h}_\beta^1(j) = 1 + \beta_1(j)\left(1 - U_1(j)\right) = 1 + \beta_1(j)\,\omega_N^j\tilde{g}(j) \tag{4.2}$$

$$h^1(j) = 1 + U_1(j) = \frac{2\left(\cos\frac{j\pi}{N}\right)^{2r}}{\left(\cos\frac{j\pi}{N}\right)^{2r} + \left(\sin\frac{j\pi}{N}\right)^{2r}},\ j \in 0, \ldots, : N, \tag{4.3}$$

$$g_\beta^1(j) = \omega_N^{-j}\left(1 - \beta_1(j)\left(1 + U_1(j)\right)\right) = \omega_N^{-j}\left(1 - \beta_1(j)\,h(j)\right) \tag{4.4}$$

Then the decomposition and reconstruction formulas of the primal scheme can be represented as follows:

$$\widehat{e}_1^u(j) = \frac{1}{2}\left(\overline{\tilde{h}_\beta^1(j)}\,\widehat{z}(j) + \overline{\tilde{h}_\beta^1(j+m)}\,\widehat{z}(j+m)\right) \tag{4.5}$$

$$\widehat{d}_1^u(j) = \frac{1}{2}\left(\overline{\tilde{g}^1(j)}\,\widehat{z}(j) + \overline{\tilde{g}^1(j+m)}\,\widehat{z}(j+m)\right) \tag{4.6}$$

$$\widehat{z}(j) = h^1(j)\widehat{e}_1^u(j) + g_\beta^1(j)\,\widehat{d}_1^u(j). \tag{4.7}$$

Proof: We start with the primal decomposition formula (4.6). Let us modify Eq. (3.1) using the identities:

$$\widehat{e}_1(j) = \frac{1}{2}\Big(\widehat{z}(j) + \widehat{z}(j+m)\Big) \quad \widehat{d}_1(j) = \frac{\omega_N^j}{2}\Big(\widehat{z}(j) - \widehat{z}(j+m)\Big) \tag{4.8}$$

So, we have:

$$\begin{aligned} \widehat{d}_1(j) &= \frac{\omega_N^j}{2}\Big(\widehat{z}(j) - \widehat{z}(j+m) - U_1(j)\Big(\widehat{z}(j) + \widehat{z}(j+m)\Big)\Big) \\ &= \frac{\omega_N^j}{2}\Big(\widehat{z}(j)\Big(1 - U_1(j)\Big) - \widehat{z}(j+m)\Big(1 + U_1(j)\Big)\Big). \end{aligned} \tag{4.9}$$

To obtain (4.6), it is sufficient to note that the function $\tilde{g}^1$, defined in (4.1), possesses the property $\tilde{g}^1(j+m) = -\omega_N^j\Big(1 + U_1(j)\Big)$. Thus we see that (4.9) is equivalent to (4.6).

To prove (4.5) we use the identity (4.8) and the already proved relation (4.6). Moreover, we recall that $\omega_N^{-(j+m)}\beta_1(j+m) = \omega_N^{-j}\beta_1(j)$. Then the decomposition formula (3.2) can be rewritten as

$$\begin{aligned} \widehat{e}_1^u(j) &= \frac{1}{2}\Big(\widehat{z}(j) + \widehat{z}(j+m)\Big) + \frac{\beta_1(j)\omega_N^{-j}}{2}\Big(\overline{\tilde{g}^1(j)}\,\widehat{z}(j) + \overline{\tilde{g}^1(j+m)}\,\widehat{z}(j+m)\Big) \\ &= \frac{1}{2}\Big(\widehat{z}(j)(1 + \beta_1(j)\omega_N^{-j}\overline{\tilde{g}^1(j)}) + \widehat{z}(j+m)(1 + \beta_1(j+m)\omega_N^{-(j+m)}\overline{\tilde{g}^1(j+m)})\Big). \end{aligned}$$

Hence, (4.5) follows.

To verify the reconstruction formula (4.7), we substitute (3.3) and (3.5) into (3.6). ■

We call the sequences $\{\tilde{h}_\beta^1(j)\}$ and $\{\tilde{g}^1(j)\}$, $j = 0, \ldots N-1$, the low-pass and high-pass decomposition filters of the first level, respectively. We call the sequences $\{h^1(j)\}$ and $\{g_\beta^1(j)\}$ the low-pass and high-pass reconstruction filters of the first level, respectively. These four filter sequences form a perfect reconstruction filter bank (Ref. 12). The following assertion is readily verified.

THEOREM 4.2. *With any $N-$periodic sequence $\beta^1(j)$, that is subject to the condition $\beta^1(j+m) = -\beta^1(j)$, the functions $\{\tilde{h}_\beta^1(j)\}$, $\tilde{g}^1(j)\}$, $\{h^1(j)\}$ and $g_\beta^1(j)\}$ satisfy the perfect reconstruction conditions*

$$h^1(j)\,\overline{\tilde{h}_\beta^1(j)} + g_\beta^1(j)\,\overline{\tilde{g}^1(j)} = 2 \tag{4.10}$$

$$h^1(j)\,\overline{\tilde{h}_\beta^1(j+m)} + g_\beta^1(j)\,\overline{\tilde{g}^1(j+m)} = 0. \tag{4.11}$$

Similar facts hold for the dual transforms. The dual decomposition filters coincide (up to constant factors) with the reconstruction filters and vice versa:

$$\tilde{H}^1(j) = h^1(j)/2,\ \tilde{G}_\beta^1(j) = g_\beta^1(j), \quad H_\beta^1(j) = 2\tilde{h}_\beta^1(j),\ G^1(j) = \tilde{g}^1(j). \tag{4.12}$$

Remark. ¿From Eqs. (4.12) and (4.3) one can observe that the dual decomposition filter $\tilde{H}^1(j)$ and the primal reconstruction filter $h^1(j)$ are equal to the magnitude squared frequency-response function of the discrete-time low-pass half-band Butterworth filter of order $2r$. From Eqs. (4.12) and (4.1) it follows that the primal decomposition filter $\tilde{g}^1(j)$ and the dual reconstruction filter $G^1(j)$ multiplied by ω_N^j are equal to the magnitude squared function of the high-pass half-band Butterworth filter Ref. 10. It means that application of these filters on a signal is equivalent to application of two passes (forward and backward) of the corresponding Butterworth filters.

4.2. Bases for the signal space

The perfect reconstruction filter banks, that were constructed above, are associated with the biorthogonal pairs of bases in the space $\mathcal{S}$ of $N-$periodic discrete signals.

Notation:

$$\varphi^1(l) = \frac{1}{N}\sum_{j=0}^{N-1} e^{\frac{2\pi ijl}{N}} h^1(j) \qquad \psi^1_\beta(l) = \frac{1}{N}\sum_{j=0}^{N-1} e^{\frac{2\pi ijl}{N}} g^1_\beta(j) \tag{4.13}$$

$$\tilde{\varphi}^1_\beta(l) = \frac{1}{N}\sum_{j=0}^{N-1} e^{\frac{2\pi ijl}{N}} \tilde{h}^1_\beta(j) \qquad \tilde{\psi}^1(l) = \frac{1}{N}\sum_{j=0}^{N-1} e^{\frac{2\pi ijl}{N}} \tilde{g}^1(j). \tag{4.14}$$

DEFINITION 4.3. *The functions φ^1 and ψ^1_β given by (4.13), which belong to the space $\mathcal{S}$, are called the low-frequency and high-frequency reconstruction wavelets of the first scale, respectively. The functions $\tilde{\varphi}^1_\beta$ and $\tilde{\psi}^1$ given by (4.13), which belong to the space $\mathcal{S}$, are called the low-frequency and high-frequency decomposition wavelets of the first scale respectively.*

Note that the wavelets in Eqs. (4.13) and (4.14) are the IDFT of the corresponding filters.

THEOREM 4.4. *The shifts of wavelets defined by eqs. (4.13) and (4.14) form a biorthogonal pairs of bases in the space $\mathcal{S}$. This means that any signal $\mathbf{z} \in \mathcal{S}$ can be represented as:*

$$z(l) = \sum_{k=0}^{m-1} e^u_1(k)\,\varphi^1(l-2k) + \sum_{k=0}^{m-1} d^u_1\,\psi^1_\beta(l-2k). \tag{4.15}$$

The coordinates $e^u_1(k)$ and $d^u_1(k)$ are the IDFT of the arrays $\widehat{e}^u_1(k)$ and $\widehat{d}^u_1(k)$ respectively and can be represented as the inner products:

$$\begin{aligned} e^u_1(k) &= \langle \mathbf{z}, \tilde{\varphi}^1_{\beta,k}\rangle, \quad \textit{where } \tilde{\varphi}^1_{\beta,k}(l) = \tilde{\varphi}^1_\beta(l-2k) \\ d^u_1(k) &= \langle z^{j+1}, \tilde{\psi}^1_k\rangle, \quad \textit{where } \tilde{\psi}^1_k(l) = \tilde{\psi}^1(l-2k). \end{aligned} \tag{4.16}$$

Proof: We start with the reconstruction formula (4.7) which we rewrite as:

$$\widehat{z}(j) = \widehat{z}_h(j) + \widehat{z}_g(j) \text{ where } \widehat{z}_h(j) = h^1(j)\widehat{e}^u_1(j) \text{ and } \quad \widehat{z}_g(j) = g^1_\beta(j)\,\widehat{d}^u_1(j).$$

We have

$$\begin{aligned} z_h(l) &= \frac{1}{N}\sum_{j=0}^{N-1} e^{\frac{2\pi ijl}{N}} h^1(j) \sum_{k=0}^{m-1} e^{\frac{-2\pi ijk}{m}} e^u_1(k) \\ &= \sum_{k=0}^{m-1} e^u_1(k)\frac{1}{N}\sum_{j=0}^{N-1} e^{\frac{2\pi ij(l-2k)}{N}} h^1(r) = \sum_{k=0}^{N-1} e^u_1(k)\,\varphi^1(l-2k). \end{aligned}$$

Similarly, we derive the relation

$$z_g(l) = \sum_{k=0}^{m-1} d^u_1\,\psi^1_\beta(l-2k).$$

The decomposition formula (4.5) implies that

$$e^u_1(k) = \frac{1}{N}\sum_{j=0}^{N-1} e^{\frac{2\pi ijk}{m}} \overline{\tilde{h}^1_\beta(j)}\,\widehat{z}(j) = e^u_1(k) = \langle \mathbf{z}, \tilde{\varphi}^1_{\beta,k}\rangle.$$

Similarly, Eq. (4.16) is derived. ■

COROLLARY 4.5. *The following biorthogonal relations hold:*

$$\langle \tilde{\varphi}^1_{\beta,k}, \varphi^1_l\rangle = \langle \psi^1_{\beta,k}, \tilde{\psi}^1_l\rangle = \delta^l_k, \quad \langle \tilde{\varphi}^1_{\beta,k}, \psi^1_{\beta,l}\rangle = \langle \tilde{\psi}^1_l, \varphi^1_k\rangle = 0, \quad \forall l,\, k.$$

Remark. The decomposition wavelets of the dual scheme are the reconstruction wavelets for the primal scheme and vice versa.

4.3. Choosing the control filter

So far we did not specify the filter sequence $\beta_1(j)$, which occurs while construction of the primal filters $g^1_\beta(j)$ and $\tilde{h}^1_\beta(j)$ and the dual ones $\tilde{G}^1_\beta(j)$ and $H^1_\beta(j)$. The only requirement was $\beta^1(j+m) = -\beta^1(j)$. Therefore, we are free to use this function for custom design of these filters and the corresponding wavelets. We present two possible approaches for choosing the control filter $\beta_1(j)$.

1. Retaining the maximal flatness of the filters As was mentioned above, the dual decomposition filter $\tilde{H}^1(j)$ (the primal reconstruction filter $h^1(j)$) and the primal decomposition filter $\tilde{g}^1(j)$ (the dual reconstruction filter $G^1(j)$) multiplied by ω_N^j are equal to the magnitude squared frequency-response functions of the discrete-time low- and high-pass half-band Butterworth filters of order $2r$, respectively. These filters are linear phase and maximally flat in their pass- and stop-bands due to the factors $\left(\cos\frac{j\pi}{N}\right)^{2r}$ for the low-pass filters and $\left(\sin\frac{j\pi}{N}\right)^{2r}$ for the high-pass filters. In Figure 1 we display these filters and the wavelets φ^1 and $\tilde{\psi}^1$ which are related to them. We will retain similar properties for filters which depend on β_1.

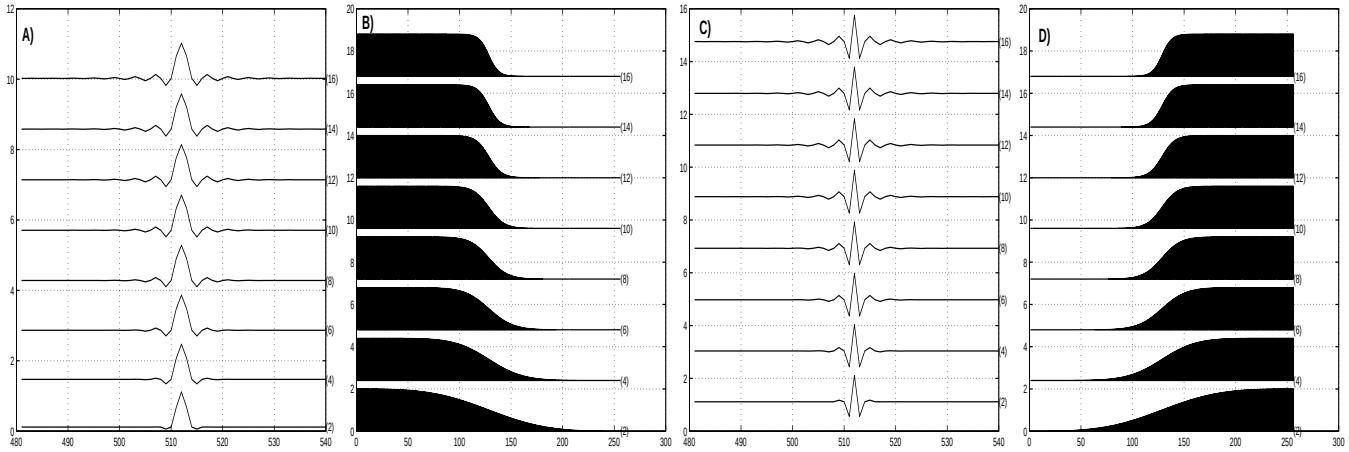

Figure 1. A) low-frequency reconstruction wavelets φ^1 of order $r = 1$ at the bottom to order $r = 8$ at the top. B) The Fourier transforms of A) which are the filters h^1. C) The high-frequency decomposition wavelets $\tilde{\psi}^1$. D) The filters $\tilde{g}^1$ for the wavelet of order r.

An easy way to achieve this is to put

$$\beta_1(j) = B^1_1(j) = U_1(j)/2 = \frac{1}{2}\frac{\left(\cos\frac{j\pi}{N}\right)^{2r} - \left(\sin\frac{j\pi}{N}\right)^{2r}}{\left(\cos\frac{j\pi}{N}\right)^{2r} + \left(\sin\frac{j\pi}{N}\right)^{2r}}. \tag{4.17}$$

Then we have

$$\tilde{h}^1_\beta(j) = 1 + \frac{1}{2}U_1(j)\Big(1 - U_1(j)\Big) = \frac{\left(\cos\frac{j\pi}{N}\right)^{2r}\left(1 + 3\left(\sin\frac{j\pi}{N}\right)^{2r}\right)}{\left(\left(\cos\frac{j\pi}{N}\right)^{2r} + \left(\sin\frac{j\pi}{N}\right)^{2r}\right)^2} \tag{4.18}$$

$$g^1_\beta(j) = \omega_N^{-j}\left(1 - \frac{1}{2}U_1(j)\Big(1 + U_1(j)\Big)\right) = \frac{\omega_N^{-j}\left(\sin\frac{j\pi}{N}\right)^{2r}\left(1 + 3\left(\cos\frac{j\pi}{N}\right)^{2r}\right)}{\left(\left(\cos\frac{j\pi}{N}\right)^{2r} + \left(\sin\frac{j\pi}{N}\right)^{2r}\right)^2} \tag{4.19}$$

We conclude from (4.18) and (4.19) that, as the filters $h^1(j)$ and $\tilde{g}^1(j)$, the filters $\tilde{h}^1_\beta(j)$, $g^1_\beta(j)$ are the mirrored replicas of each other. We display these filters and the corresponding wavelets in Figure 2. We observe that the

filters and the wavelets are similar to the previous ones but the flatness of the filters is disturbed by the bumps near the cut-off. These bumps appear due to the factors $1+3\left(\sin\frac{j\pi}{N}\right)^{2r}$ and $1+3\left(\cos\frac{j\pi}{N}\right)^{2r}$ in (4.18) and (4.19) respectively.

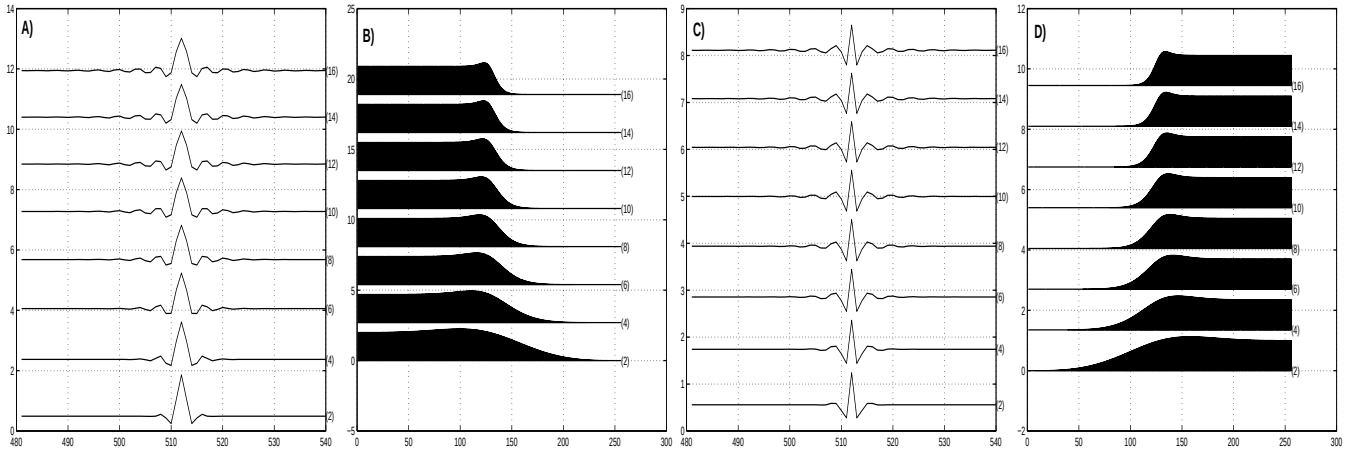

Figure 2. A) low-frequency decomposition wavelets $\tilde{\varphi}^1_\beta$ of order $r=1$ at the bottom to order $r=8$ at the top. B) The Fourier transforms of A) which are the filters $\tilde{h}^1_\beta$. C) The high-frequency reconstruction wavelets ψ^1_β. D) The filters g^1_β for the wavelet of order r. The control filter $\beta_1(j)=U^1(j)/2$.

2. Orthogonality of the wavelets: Another suggestion for the choice of β is triggered by the following consideration. Generally, the high- and low-frequency wavelets $\varphi^1(l)$ and $\psi^1_\beta(l)$, respectively, are not orthogonal to each other, as well as $\tilde{\varphi}^1_\beta(l)$ and $\tilde{\psi}^1(l)$. But, by proper choice of the control filter $\beta_1(j)$ we can get this property. In this case the signals $\mathbf{z}_h$ and $\mathbf{z}_g$, in the representation $\mathbf{z}=\mathbf{z}_h+\mathbf{z}_g$, become orthogonal to each other. By this means we are able to remarkably reduce the redundancy which is inherent to the biorthogonal wavelet transforms. Moreover, the decomposition wavelets $\tilde{\varphi}^1_{\beta,k}$ belong to the same subspace that the reconstruction wavelets φ^1_l belong to. The wavelets $\tilde{\varphi}^1_{\beta,k}$ can be expressed as linear combinations of the wavelets φ^1_l and vice versa. The same is true for the high-pass wavelets $\tilde{\psi}^1_k$ and $\psi^1_{\beta,l}$.

PROPOSITION 4.6. *If the control filter $\beta^1(j)$ is chosen as*

$$\beta_1(j)=B^2_1(j)=\frac{U_1(j)}{1+(U_1(j))^2}=\frac{1}{2}\frac{\left(\cos\frac{j\pi}{N}\right)^{4r}-\left(\sin\frac{j\pi}{N}\right)^{4r}}{\left(\cos\frac{j\pi}{N}\right)^{4r}+\left(\sin\frac{j\pi}{N}\right)^{4r}} \tag{4.20}$$

then the following orthogonal relations hold

$$\langle\psi^1_{\beta,k},\varphi^1_l\rangle=\langle\tilde{\varphi}^1_{\beta,k},\tilde{\psi}^1_l\rangle=0,\quad\forall l,\,k. \tag{4.21}$$

We display the filters and the corresponding wavelets in Figure 2. We observe that the filters and the wavelets are similar to the filters and wavelets with $\beta_1(j)=U^1(j)/2$ but now the bumps are more visible and the cut-offs are steeper than before. The wavelets are somewhat smoother but fail in spatial localization.

Remark. When we doubled the order of the filer $B^1_1(j)$, which is given by (4.17), we get the filter $B^2_1(j)$.

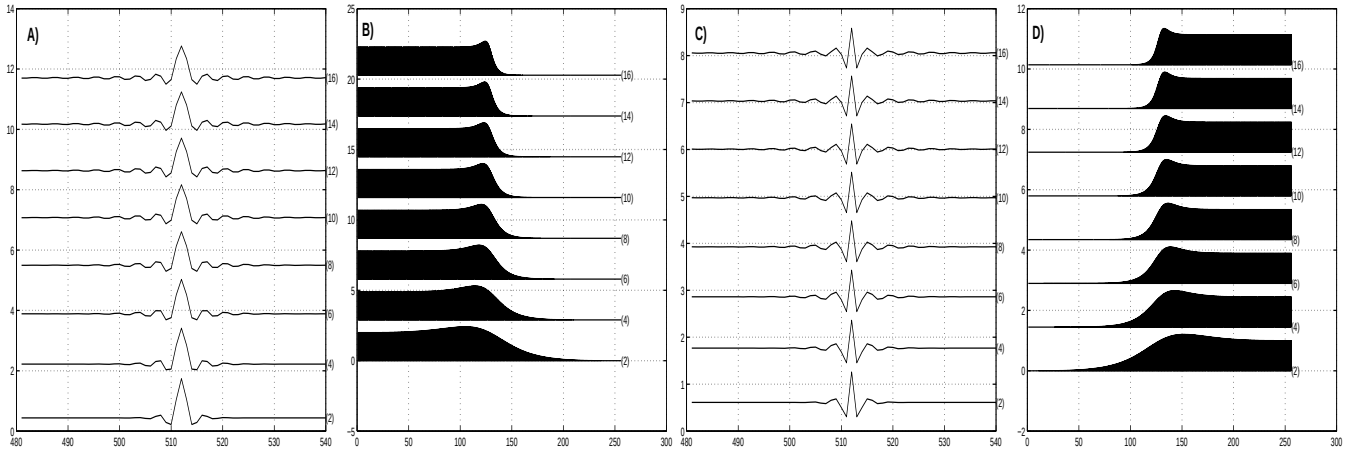

Figure 3. A) low-frequency decomposition wavelets $\tilde{\varphi}_b^1$ of order $r = 1$ at the bottom to order $r = 8$ at the top. B) The Fourier transforms of A) which are the filters $\tilde{h}_b^1$. C) The high-frequency reconstruction wavelets ψ_b^1. D) The filters g_b^1 for the wavelet of order r. The control filter $\beta_1(j) = U^1(j)/(1 + (U^1(j)^2)$.

Proof: Using (4.13) we can write

$$\begin{aligned}\langle \psi_{\beta,k}^1, \varphi_l^1 \rangle &= \frac{1}{N^2} \sum_{n=0}^{N-1} \sum_{j=0}^{N-1} e^{-\frac{2\pi i j(n-2l)}{N}} \overline{h^1(j)} \sum_{s=0}^{N-1} e^{\frac{2\pi i s(n-2k)}{N}} g_\beta^1(s) \\ &= \frac{1}{N^2} \sum_{j,s=0}^{N-1} \overline{h^1(j)}\, g_\beta^1(s) e^{\frac{2\pi i 2(ks-jl)}{N}} \sum_{n=0}^{N-1} e^{-\frac{2\pi n(s-j)}{N}} = \frac{1}{N} \sum_{j=0}^{N-1} \overline{h^1(j)}\, g_\beta^1(j) \omega_m^{j(k-l)}.\end{aligned}$$

Since the function $\omega_m^{j(k-l)}$ is $m-$periodic with respect to j, we represent the inner product as follows

$$\langle \psi_{\beta,k}^1, \varphi_l^1 \rangle = \sum_{j=0}^{m-1} \omega_m^{j(k-l)} \left(\overline{h^1(j)}\, g_\beta^1(j) + \overline{h}^1(j+m)\, g_\beta^1(j+m) \right).$$

Equations (4.1) and (4.2) imply that

$$\begin{aligned}\overline{h^1(j)}\, g_\beta^1(j) &= \omega_m^{-j/2} \left((1 + U_1(j))(1 - \beta^1(j) \left(1 + U_1(j)\right) \right), \\ \overline{h^1(j+m)}\, g_\beta^1(j+m) &= -\omega_m^{-j/2} \left((1 - U_1(j))(1 + \beta^1(j) \left(1 - U_1(j)\right) \right).\end{aligned}$$

Hence, we have

$$\langle \psi_{\beta,k}^1, \varphi_l^1 \rangle = \sum_{j=0}^{m-1} \omega_m^{j(k-l-1/2)} \left(2U_1(j) - 2\beta^1(j) \left(1 + (U_1(j))^2\right) \right).$$

Substitution of (4.20) results in $\langle \psi_{\beta,k}^1, \varphi_l^1 \rangle = 0$. The second relation in (4.21) is similarly proved.■

5. MULTISCALE WAVELET TRANSFORMS

Repeated applications of the transform can be achieved in an iterative way as was presented above. It can be implemented as either a linear invertible transform of a wavelet type or as a wavelet packet type transform which results in an overcomplete representation of the signal. We explain one multiscale advance of the wavelet transform.

In this transform we store the array $\mathbf{d}_1^u$ and decompose the array $\mathbf{e}_1^u$. Actually, we employ the DFT arrays $\widehat{\mathbf{e}}_1^u$ and $\widehat{\mathbf{d}}_1^u$ which were derived in the previous step. The IDFT is applied on the array $\widehat{\mathbf{d}}_1^u$ that yields $\mathbf{d}_1^u$.

Let $\mathbf{e}_2^u$ and $\mathbf{d}_2^u$ denote the even and odd sub-arrays of the array $\mathbf{e}_1^u$. We can find the values of the corresponding DFT directly from $\widehat{\mathbf{e}}_1^u$:

$$\widehat{e}_2(j) = (\widehat{e}_1^u(j) + (\widehat{e}_1^u(j+m/2))/2 \quad \widehat{d}_2(j) = \omega_{N/2}^j\,(\widehat{e}_1^u(j) + (\widehat{e}_1^u(j+m/2))/2.$$

The filters for the first step of the transform were produced from the function U_1 (see (2.5)). The filters for the second step we produce using the new function U_2 , which is the downsampled version of U_1: $U_2(j) = U_1(2j)$. (see (2.5)).

The decomposition steps for the primal scheme are:

1. $\widehat{d}_2^u(j) = \widehat{d}_2(j) - \omega_{N/2}^j\,\widehat{e}_2(j)U_2(j)$
2. $\widehat{e}_2^u(j) = \widehat{e}_2(j) + \beta^2(j)\,w_{N/2}^{-j}\,\widehat{d}_2^u(j)$
3. The array $\mathbf{d}_2^u$ is derived by the application of the IDFT. If we terminate the decomposition at this step, we apply IDFT on $\widehat{\mathbf{e}}_2^u$ as well and produce $\mathbf{e}_2^u$. In this event, the original array $\mathbf{z}$ is transformed into the array $\{\mathbf{d}_1^u,\ \mathbf{d}_2^u,\ \mathbf{e}_2^u\}$. To proceed in getting coarser scales in the decomposition we use the array $\widehat{\mathbf{e}}_2^u$ rather than $\mathbf{e}_2^u$.

The reconstruction steps are:

1. Apply the DFT on $\mathbf{d}_2^u$. If $\widehat{\mathbf{e}}_2^u$ is not available from the previous steps of the reconstruction, apply it on $\mathbf{e}_2^u$.
2. $\widehat{e}_2(j) = \widehat{e}_2^u(j) - \beta^2(j)\,w_{N/2}^{-j}\,\widehat{d}_2^u(j)$
3. $\widehat{d}_2(j) = \widehat{d}_2^u(j) + \omega_{N/2}^j\,\widehat{e}_2(j)U_2(j)$
4. $\widehat{e}_2(j) = \widehat{e}_2(j) + \omega_{N/2}^{-j}\widehat{d}_2(j)$

The dual scheme is implemented in a similar manner.

The described transform is linked with the $N/2$-periodic filters $\tilde{g}^2(j),\ \tilde{h}_\beta^2(j),\ h^2(j),\ g_\beta^2(j)$, which are the downsampled versions of the corresponding filters of the first step. It is worth noting that the filters $\tilde{g}^2(j)$ and $h^2(j)$ are two-pass quarter-band Butterworth filters. The filters $\tilde{h}_\beta^2$ and $\tilde{g}^2$ are applied on the array $\widehat{\mathbf{e}}_1^u$ to derive $\widehat{\mathbf{e}}_2^u$ and $\widehat{\mathbf{d}}_2^u$. Conversely, h^2 and g_β^2 are applied on the arrays $\widehat{\mathbf{e}}_2^u$ and $\widehat{\mathbf{d}}_2^u$ to restore $\widehat{\mathbf{e}}_1^u$.

The transform can be viewed as an expansion of the signal with biorthogonal pair of bases:

$$z(l) = \sum_{k=0}^{m/2-1} e_2^u(k)\,\varphi^2(l-4k) + \sum_{k=0}^{m/2-1} d_2^u(k)\,\psi_\beta^2(l-4k) + \sum_{k=0}^{m-1} d_1^u(k)\,\psi_\beta^1(l-2k), \tag{5.1}$$

where low-pass and high-pass reconstruction wavelets of the second scale are defined as follows:

$$\varphi^2(l) = \frac{1}{N}\sum_{j=0}^{N-1} e^{\frac{2\pi i j l}{N}} h^1(j)h^2(j), \quad \psi_\beta^2(l) = \frac{1}{N}\sum_{j=0}^{N-1} e^{\frac{2\pi i j l}{N}} h^1(j)g_\beta^2(j).$$

The coordinates in (5.1) are inner products with 4-sample shifts of the decomposition wavelets of the second scale:

$$\tilde{\varphi}_\beta^2(l) = \frac{1}{N}\sum_{j=0}^{N-1} e^{\frac{2\pi i j l}{N}} \tilde{h}_\beta^1(j)\tilde{h}_\beta^2(j), \quad \tilde{\psi}_\beta^2(l) = \frac{1}{N}\sum_{j=0}^{N-1} e^{\frac{2\pi i j l}{N}} \tilde{h}_\beta^1(j)\tilde{g}^2(j).$$

In Figure 4 we display wavelets of order 1 up to the fourth level and their spectra. Note that these wavelets are compactly supported and have 2 vanishing moments. In Figure 5 we display wavelets of order 10 up to the fourth level and their spectra. These wavelets are outperformed by the wavelets of lower orders in spatial localization but win in frequency localization and smoothness. Unlike the mechanism in the wavelet transform, in the wavelet packet transform both sub-arrays $\mathbf{e}_1^u$ and $\mathbf{d}_1^u$ of the first scale are subject to the decomposition that produces four second-scale sub-arrays. In turn, these four arrays produce eight sub-arrays for the third scale, and so on. All sub-arrays which are related to a certain scale are stored.

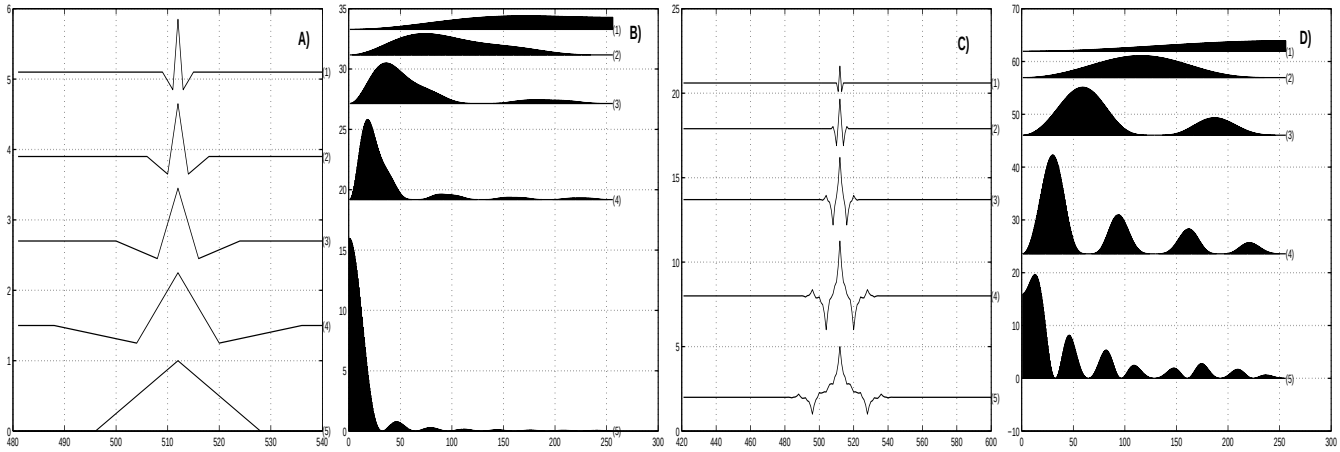

Figure 4. A) Reconstruction wavelets ψ^l_β, $l = 1 \dots 4$ of order 1 (lines 1–4) and φ^l, $l = 4$ (line 5) B) Their spectra C) Decomposition wavelets $\tilde{\psi}^l_\beta$, $l = 1 \dots 4$ of order 1 (lines 1-4) and $\tilde{\varphi}^l_\beta$, $l = 4$ (line 5) D) Their spectra.

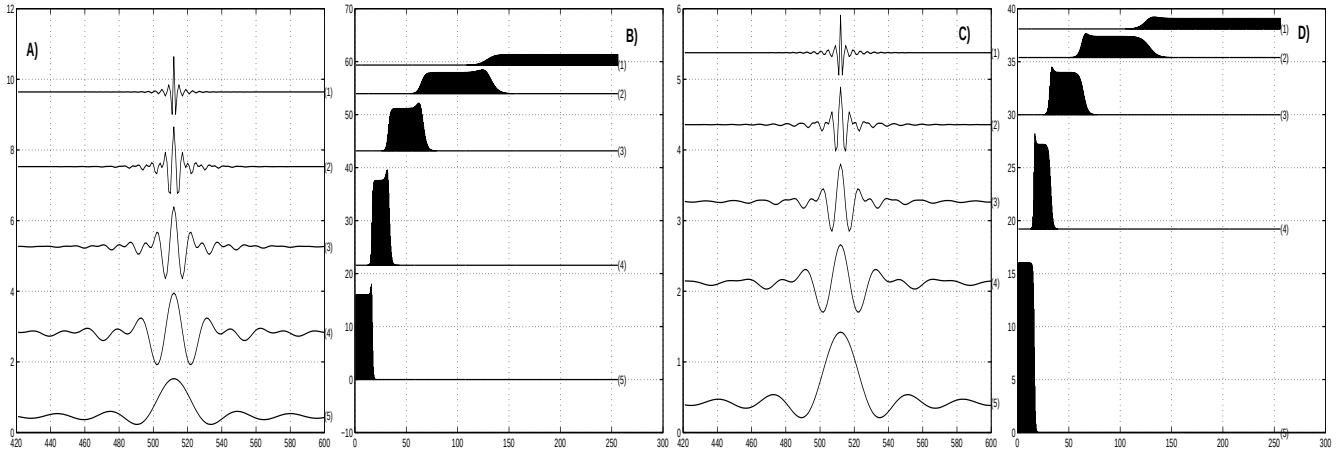

Figure 5. A) Reconstruction wavelets ψ^l_β, $l = 1 \dots 4$ of order 10 (lines 1–4) and φ^l, $l = 4$ (line 5) B) Their spectra C) Decomposition wavelets $\tilde{\psi}^l_\beta$, $l = 1 \dots 4$ of order 1 (lines 1-4) and $\tilde{\varphi}^l_\beta$, $l = 4$ (line 5) D) Their spectra.

6. CONCLUSIONS

We presented a new family of biorthogonal wavelet transforms and a related library of biorthogonal periodic symmetric waveforms. For the construction we used the interpolatory discrete splines which enabled us to design a library of perfect reconstruction filter banks. These filter banks are intimately related to Butterworth filters.

The construction is performed in a "lifting" manner that allows more efficient implementation and provides tools for custom design of the filters and wavelets. As it is common in lifting schemes, the computations can be carried out "in place" and the inverse transform is performed in a reverse order. The difference with the conventional lifting scheme Ref. 13 is that all the transforms are implemented in the frequency domain with the use of the fast Fourier transform (FFT). However, the time-domain implementation is possible by means of recursive IIR filtering similar to the implementation of the Butterworth filters.

We suggested two ways to choose the control filters which are inherent in the transforms. However, many more ways are possible. This subject deserves a special investigation.

High-frequency filters of an order r in our construction comprise the factor $\left(\sin \frac{j\pi}{N}\right)^{2r}$. In a non-periodic setting it corresponds to the vanishing moments property up to order $2r$ of the corresponding wavelets. Thus, such a filter

turns fragments of the signal , which (almost) coincide with polynomial of degree p, close to zero. The low-frequency filters, on the contrary, leave the fragments almost intact.

Our algorithm allows a stable construction of filters comprising these sine-blocks of practically any orders.

The computational complexity of the application of the wavelet transform on a signal of length N is the same as the application of the FFT on the signal which is $O(N \log_2 N)$. Increase of the order in our scheme does not affect the cost of the implementation. Therefore, especially for higher orders r, the complexity of our algorithm is comparable if not less than the complexity of the standard wavelet transform.

We should particularly emphasize that our scheme is based on interpolation and, as such, it involves only samples of signals and it does not require any use of quadrature formulas. This property is valuable for digital signal and image processing.

Also of great importance to these applications is the fact that these filters have linear phase property and the basic waveforms are symmetric. In addition, these filters yield perfect frequency resolution.

We anticipate a wide range of applications for the presented library of waveforms in signal and image processing.

REFERENCES

1. A. Aldroubi, M. Eden and M. Unser, "Discrete spline filters for multiresolutions and Wavelets of l_2", *SIAM Math. Anal.,* **25**, (1994), 1412-1432.
2. Battle G., " A block spin construction of ondelettes. Part I. Lemarié functions", *Comm. Math. Phys.* **110**(1987), 601-615.
3. C. K. Chui and J. Z. Wang, " On compactly supported spline wavelets and a duality principle", *Trans. Amer. Math. Soc.* **330**(1992), 903-915.
4. A. Cohen, I. Daubechies and J.-C. Feauveau, " Biorthogonal bases of compactly supported wavelets", *Commun. on Pure and Appl. Math.* **45** (1992), 485-560.
5. D. L. Donoho, "Interpolating wavelet transform,", *Preprint 408,* Department of Statistics, Stanford University, 1992.
6. C. Herley and M. Vetterli, "Wavelets and recursive filter banks", *IEEE Trans. Signal Proc.,* **41(12)** (1993), 2536-2556.
7. Lemarié P.G., " Ondelettes à localization exponentielle", *J. de Math. Pures et Appl.* **67**(1988), 227-236.
8. Malozemov, V. N.; Pevnyi, A. B.; Tretyakov, A. A. "A fast wavelet transform for discrete periodic signals and images ".*Problems Inform. Transmission* **34** (1998), no. 2, 161–168.
9. V. N. Malozemov, and A. B. Pevnyi, "Discrete periodic splines and their numerical application", *Comp. Mathematics and Math. Physics,* **38**, (1998), 1181-1192.
10. A. V. Oppenheim, R. W. Shafer, *Digital signal processing*, Englewood Cliffs, New York, Prentice Hall, 1989.
11. A. B. Pevnyi and V. A. Zheludev, "On wavelet analysis in the discrete splines space", *Proceedings Second Int. Conf. "Tools for math. modelling99".* V.4. St. Petersburg: SPTU, 1999, pp. 181-195.
12. G. Strang, and T. Nguen, *Wavelets and filter banks*, Wellesley-Cambridge Press, 1996.
13. W. Sweldends "The lifting scheme: A custom design construction of biorthogonal wavelets", *Appl. Comput. Harm. Anal.* **3(2)**, (1996), 186-200.
14. V. A. Zheludev, "Periodic splines, harmonic analysis, and wavelets" in *Signal and image representation in combined spaces,* , Wavelet Anal. Appl., 7," (eds. Y. Y. Zeevi and R. Coifman), Academic Press, San Diego, CA, 1998, pp. 477–509.
15. Zheludev V.A., Averbuch A.Z. "A biorthogonal wavelet scheme based on interpolatory splines", *Proceedings Second Int. Conf. "Tools for math. modelling99",* V. 4. St. Petersburg: SPTU, 1999, pp .214–231.